

Spectroscopy of  $^{186}\text{Pb}$  with mass identification

A. M. Baxter and A. P. Byrne

*Department of Physics and Theoretical Physics, Faculty of Science, Australian National University, Canberra ACT 0200, Australia*

G. D. Dracoulis

*Department of Nuclear Physics, RSPHysSE, Australian National University, Canberra ACT 0200, Australia*R. V. F. Janssens, I. G. Bearden, R. G. Henry, D. Nisius, C. N. Davids,  
T. L. Khoo, T. Lauritsen, H. Penttilä, D. J. Henderson, and M. P. Carpenter*Physics Division, Argonne National Laboratory, Argonne, Illinois 60439*

(Received 14 July 1993)

Transitions in the very neutron-deficient isotope  $^{186}\text{Pb}$  have been identified in mass-gated, recoil- $\gamma$ , and recoil- $\gamma$ - $\gamma$  coincidence data obtained with a fragment mass analyzer and Compton-suppressed Ge-detector array. The results of the present work confirm and extend a band of levels tentatively proposed in earlier work done elsewhere, and provide a definitive mass assignment of the observed transitions. The band observed in  $^{186}\text{Pb}$  bears a very close resemblance to the yrast band in the isotope  $^{184}\text{Hg}$ , supporting the view that the  $^{186}\text{Pb}$  band is built upon a prolate structure.

PACS number(s): 21.10.Re, 23.20.Lv, 27.70.+q

The first evidence for low-lying, prolate-deformed, rotational bands in the very neutron-deficient isotopes  $^{186}\text{Pb}$  and  $^{188}\text{Pb}$  was reported recently by Heese *et al.* [1]. In both these nuclei, the main feature of the level schemes is a single band with rotationlike spacing for the third and higher excited levels. The properties of this band are very much different from the comparable yrast levels observed [2] in  $^{190}\text{Pb}$  and  $^{192}\text{Pb}$  but, on the other hand, they are similar to rotational bands observed [3-5] in the corresponding isotones  $^{184}\text{Hg}$  and  $^{186}\text{Hg}$ . This led Heese *et al.* to identify the bands they observed in  $^{186}\text{Pb}$  and  $^{188}\text{Pb}$  with the prolate minimum predicted [6,7] to occur in the potential energy surface for the very light lead nuclei.

In the case of  $^{186}\text{Pb}$ , Heese *et al.* obtained a spectrum of five cascade transitions from  $\gamma$ - $\gamma$  coincidence data gated by a recoil filter detector to rescue the fusion-evaporation products from the sea of fission. Calculations with the code PACE, for the reaction  $^{154}\text{Gd} + ^{36}\text{Ar}$  reaction at 175 MeV, indicate that the fission channel accounts for approximately 85% of the total fusion cross section and the  $4n$  channel for as little as 1%. Furthermore, the competing fission channels preferentially deplete higher  $l$ -values which not only limits the spin of the evaporation residues, but reduces the cross section for producing them as well. It is therefore difficult to achieve high statistical accuracy and it is essential that background be minimized. The recoil filter detector used by Heese *et al.* rejects  $\gamma$ -radiation from fission but it does not distinguish between the potentially numerous fusion-evaporation channels. Because the proposed band structure differs so markedly from that of the even-mass Pb isotopes with  $A > 188$ , it is important that the observed  $\gamma$ -ray transitions be correctly and unambiguously attributed to  $^{186}\text{Pb}$ . In the work reported here, we set out to establish the  $\gamma$ -decay scheme of  $^{186}\text{Pb}$  by detecting

$\gamma$ - $\gamma$  coincidences gated by a recoil mass spectrometer to provide definitive mass identification.

Excited levels of  $^{186}\text{Pb}$  were populated by bombarding a  $^{154}\text{Gd}$  target with 174 MeV,  $^{36}\text{Ar}^{10+}$  ions from the ATLAS superconducting, linear accelerator at the Argonne National Laboratory. The target was a 0.38 mg/cm<sup>2</sup> thick, self-supporting, metallic foil enriched to 66.5% in  $^{154}\text{Gd}$ ; it also contained 17.5% of  $^{155}\text{Gd}$ , 7% of  $^{156}\text{Gd}$ , and 3.5% or less of each of  $^{157,158,160}\text{Gd}$ . The Argonne fragment mass analyzer (FMA) was set at 0° to the beam to accept evaporation residues recoiling from the target, and  $\gamma$ -radiation was detected by ten Compton-suppressed, germanium detectors of the Argonne - Notre Dame, BGO  $\gamma$ -ray facility placed around the target.

The FMA (Davids *et al.* [8]) is a triple-focussing, recoil mass spectrometer consisting of a symmetric combination of two electric dipoles and one magnetic dipole which produces, at its focal plane, dispersion in mass/charge of the reaction products. When the FMA is at 0°, beam particles entering it are intercepted by the anode of the first electric dipole. A 10  $\mu\text{g}/\text{cm}^2$  carbon foil was placed downstream, 3 cm from the target, to restore the equilibrium charge-state distribution of recoiling ions which may have undergone decay by internal conversion after emerging from the target, but before reaching this charge-state reset foil. Those recoiling ions which are transported to the focal plane are detected by a multiwire proportional counter (MWPC) of 15 cm by 5 cm active area. In the configuration used here, the MWPC produced signals proportional to the rate of energy loss  $\Delta E$  of the particles and to their position along the dispersive axis of the focal plane. A silicon surface-barrier detector was located in the target chamber, at 35° to the beam direction, to monitor beam intensity and target condition. The target thickness was chosen to be as large as possible without there being significant loss of transmission through the

FMA because of multiple scattering in the target.

Data were recorded in event mode and, for a valid event, the following parameters were recorded: the energy  $E_\gamma$  and time (with respect to the beam pulse) of any  $\gamma$ -rays,  $\Delta E$  and position  $X_{\text{MWPC}}$  from the MWPC, and the time between the first  $\gamma$ -ray and the MWPC  $\Delta E$  signal.

A mass spectrum of recoil ions detected at the focal plane of the FMA is shown in Fig. 1. The electric and magnetic fields of the FMA were set so that the central trajectory corresponded to mass-187 ions with a recoil energy of 29.6 MeV and an (average) charge state of 18.5. In this way, the two most abundant charge states ( $Q = 18$  and 19) of the measured charge-state distribution both fitted within the aperture of the MWPC. The spectrum in Fig. 1 was obtained by projecting onto the position axis a matrix of  $X_{\text{MWPC}}$  versus  $E_\gamma$ , in which it was required that the transit time of the ions through the FMA and the  $\Delta E$  pulse from the MWPC both correspond to evaporation residues. In constructing this and other matrices,  $\gamma$ -ray energies were corrected for Doppler shifts. The mass resolving power  $M/\Delta M$  in the spectrum (Fig. 1) is approximately 270 and is sufficient that peaks corresponding to  $A = 183$  to 187 inclusive can be clearly discerned even though they are not completely resolved. The tail on the high-mass side of the peaks arises from second-order aberrations in the FMA, which was used with maximum aperture to achieve the greatest yield.

Projections on the  $E_\gamma$  axis of the  $X_{\text{MWPC}}$  versus  $E_\gamma$  matrix produce the spectra shown in Figs. 2(a) and 2(b); Fig. 2(a) is a sum of projections from gates on the two mass-186 peaks (corresponding to the two charge states) and Fig. 2(b) is a sum of gates on the two mass-187 peaks. Most of the strong peaks in the mass-186 gate can be identified with known transitions in  $^{186}\text{Hg}$  [4,5] and  $^{186}\text{Tl}$  [9], while the mass-187 gate is dominated by lines corresponding to  $^{187}\text{Tl}$  [10]. The ability of the FMA to distinguish  $\gamma$ -rays according to the mass of the emitting nucleus is apparent. It is worth noting that a line near 662 keV is prominent in both the mass-186 and -187 gates; in the latter case it corresponds to a known transition [10] in  $^{187}\text{Tl}$ .

Figure 2(c) shows a spectrum of  $\gamma$ -rays attributed to

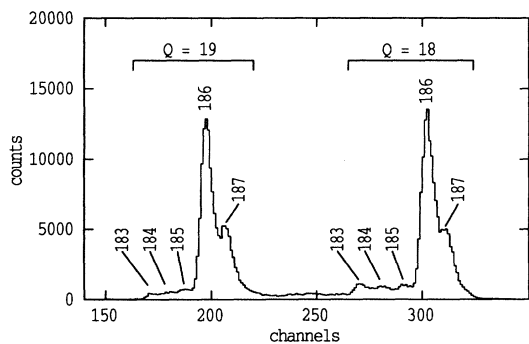


FIG. 1. Mass spectrum from projection of the  $X_{\text{MWPC}}$  versus  $E_\gamma$  matrix onto the  $X_{\text{MWPC}}$  axis. Peaks are labeled by the mass number of the recoiling ions and fall into two groups corresponding to charge states  $Q = 18$  and 19.

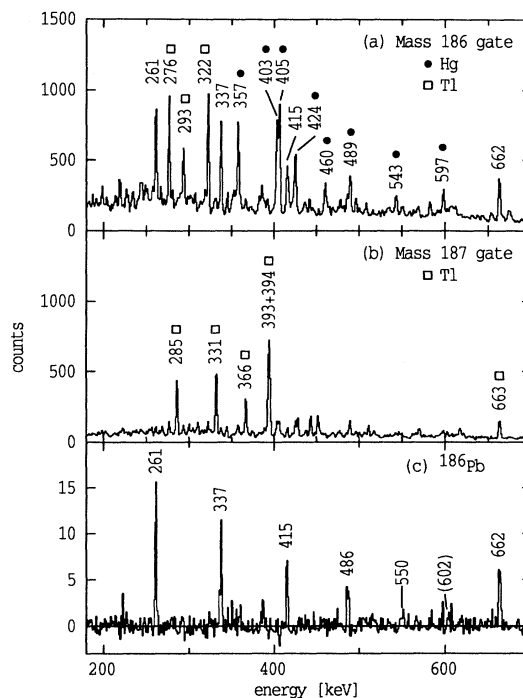


FIG. 2. (a) Part of the  $\gamma$ -ray spectrum gated by the two mass-186 peaks in the  $X_{\text{MWPC}}$  spectrum. (b) Part of the  $\gamma$ -ray spectrum gated by the two mass-187 peaks in the  $X_{\text{MWPC}}$  spectrum. (c) Sum of projections from the FMA- $E_\gamma$ - $E_\gamma$  coincidence data with gates on the 261-, 337-, 415-, and 662-keV lines, and with gates to select mass-186 evaporation residues. In all three spectra the larger peaks are labeled by their energies and the nucleus to which they are attributed if it is not  $^{186}\text{Pb}$ .

$^{186}\text{Pb}$ , obtained from the FMA- $E_\gamma$ - $E_\gamma$  coincidence data. It is a sum of projections with gates on the 261-, 337-, 415-, and 662-keV  $\gamma$ -ray lines: gates were also set on (i) the mass-186 peaks in the  $X_{\text{MWPC}}$  spectrum, (ii) the peak corresponding to evaporation residues in the MWPC  $\Delta E$  spectrum, and (iii) the evaporation-residue peak in the time-of-flight spectrum. The coincident Pb x-rays, although relatively weak owing presumably to small internal conversion coefficients, were sufficient to confirm identification of the atomic number of the emitting nuclei. Six lines, and possibly a seventh, can be seen and all but the 602-keV line show coincidences with one another in the individual gated spectra. Relative intensities of

TABLE I. Relative  $\gamma$ -ray intensities for transitions in  $^{186}\text{Pb}$ .

$E_\gamma$ (keV)	Intensity	$E_i$ (keV) <sup>a</sup>
260.6(3)	85(3)	923.0
337.0(3)	85(3)	1260.0
415.1(5)	75(4)	1675.1
485.8(5)	24(3)	2160.9
550.5(5)	18(3)	2711.4
602.5(8) <sup>b</sup>	5(3)	3313.9
662.4(5)	100(4)	662.4

<sup>a</sup>Excitation energy of initial level.

<sup>b</sup>Tentatively assigned to level scheme; see text.

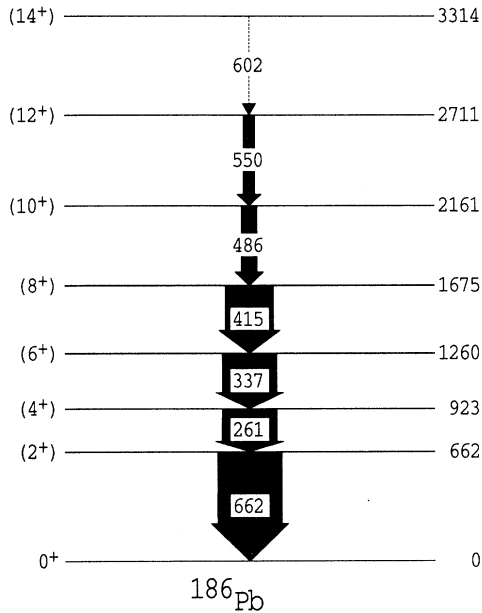


FIG. 3. Level scheme of  $^{186}\text{Pb}$  deduced in the present work. The widths of the arrows indicate the relative intensities of the corresponding  $\gamma$ -rays.

the lines are given in Table I; they were obtained from the projection of the  $X_{\text{MWPC}}$  versus singles  $\gamma$ -ray matrix with a gate on the mass-186 peaks [Fig. 2(a)]. If the  $^{186}\text{Pb}$   $\gamma$ -ray transitions are then arranged in a cascade according to the relative intensities shown in Table I, they give the level spectrum shown in Fig. 3.

The angular distributions of the  $^{186}\text{Pb}$   $\gamma$ -rays in the FMA- $\gamma$  data were isotropic within statistical uncertainties, presumably as a result of deorientation as the ions recoil in vacuum. Measurements with a thick or backed target would not permit the background reduction achievable by detecting coincidences between  $\gamma$ -rays and evaporation residues, so it was not possible to obtain information on spins or lifetimes in the present experiment. Nevertheless, the low x-ray yield is consistent with  $E2$  multipolarity for the decays, and it is assumed that the excited levels in Fig. 3 have spins and parities following the expected  $2^+, 4^+, 6^+, \dots$  sequence. Furthermore, after allowing for internal conversion, the total intensities of the 662- and 261-keV transitions are equal, consistent with the latter being  $E2$ .

The  $^{186}\text{Pb}$  level scheme deduced in the present work (Fig. 3) agrees with that of Heese *et al.* [1] up to the  $10^+$  state at 2161 keV. For the transition feeding that state we obtain  $E_\gamma = 550$  keV whereas Heese *et al.* report tentatively a transition of 532 keV. The 602-keV  $\gamma$ -ray is the weakest transition observed here. It is only seen when all coincidence spectra gated by individual  $^{186}\text{Pb}$  transitions are summed and its placement is therefore not established beyond doubt.

In Fig. 4, the dynamic moment of inertia and aligned angular momentum for the  $^{186}\text{Pb}$  level sequence given in Fig. 3 are plotted against rotational frequency  $\hbar\omega$ , together with the corresponding values for the yrast band

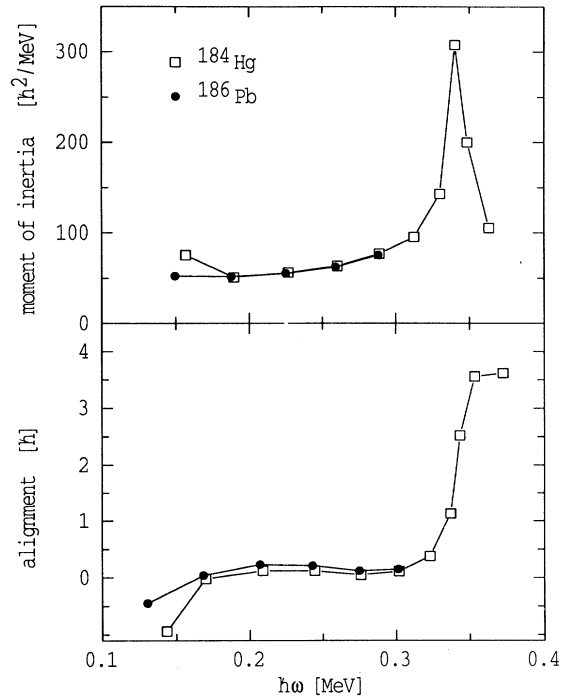


FIG. 4. Plots of aligned angular momentum and dynamic moment of inertia against rotational frequency  $\hbar\omega$  for states with  $J \geq 4$  in  $^{186}\text{Pb}$  and in the yrast band of its isotone  $^{184}\text{Hg}$ . The reference parameters for the alignment calculation were  $\mathfrak{S}_0 = 25.1\hbar^2/\text{MeV}$  and  $\mathfrak{S}_1 = 209\hbar^4/\text{MeV}^3$ .

in the isotone  $^{184}\text{Hg}$ . The  $^{184}\text{Hg}$  data were obtained from Refs. [3] and [10]. It is clear that, for  $\hbar\omega > 0.2$  MeV, the behavior of the two bands is very similar; indeed, for the cascade from  $J = 14$  to  $J = 4$ , the energies of corresponding transitions agree to within 4 keV. This similarity has been remarked upon elsewhere (e.g., [1,11]). However, with the corrected energy reported here for the  $12^+ \rightarrow 10^+$  transition and the addition, albeit tentatively, of the 602-keV transition, it can be seen that the two bands are almost identical over five transitions. This supports the view that the  $^{186}\text{Pb}$  band is built on essentially the same prolate structure assigned [3] to the  $^{184}\text{Hg}$  yrast band. It is unfortunate that the  $^{186}\text{Pb}$  band could not be observed to sufficiently high angular frequency to see whether or not it displays the same upbend seen in  $^{184}\text{Hg}$  at  $\hbar\omega \approx 0.33$  MeV.

In this investigation we have found a cascade of six  $\gamma$ -ray transitions which have been assigned to  $^{186}\text{Pb}$  by a definitive mass identification. The striking similarity of this band to the yrast band of the isotone  $^{184}\text{Hg}$  strongly confirms the conclusion of the earlier work of Heese *et al.* [1] that the  $^{186}\text{Pb}$  band, and a similar band in  $^{188}\text{Pb}$ , provide the first direct evidence for prolate deformation in the lead isotopes.

This work was supported in part by the Australian Research Council, the Australian Government's Department of Industry, Technology and Commerce and by the U.S. Department of Energy, Nuclear Physics Division, under Contract No. W-31-109-ENG-38.

- [1] J. Heese, K. H. Maier, H. Grawe, J. Grebosz, H. Kluge, W. Meczynski, M. Schramm, R. Schubart, K. Spohr, and J. Styczen, *Phys. Lett. B* **302**, 390 (1993).
- [2] C. Roulet, G. Albouy, G. Auger, J. M. Lagrange, M. Pautrak, K. G. Rensfelt, H. Richel, H. Sergolle, and J. Vanhorenbeeck, *Nucl. Phys.* **A323**, 495 (1979).
- [3] W. C. Ma, A. V. Ramayya, J. H. Hamilton, S. J. Robinson, J. D. Cole, E. F. Zganjar, E. H. Spejewski, R. Bengtsson, W. Nazarewicz, and J.-Y. Zhang, *Phys. Lett.* **167B**, 277 (1986).
- [4] W. C. Ma, J. H. Hamilton, A. V. Ramayya, L. Chaturvedi, J. K. Deng, W. B. Gao, Y. R. Chang, J. Kormicki, X. W. Zhao, N. R. Johnson, J. D. Garrett, I. Y. Lee, C. Baktash, F. K. McGowan, W. Nazarewicz, and R. Wyss, *Phys. Rev. C* **47**, R5 (1993).
- [5] M. G. Porquet, G. Bastin, C. Bourgeois, A. Korichi, N. Perrin, H. Sergolle, and F. A. Beck, *J. Phys. G: Nucl. Part. Phys.* **18**, L29 (1992).
- [6] F. R. May, V. V. Pashkevich, and S. Frauendorf, *Phys. Lett.* **68B**, 113 (1977).
- [7] R. Bengtsson and W. Nazarewicz, *Z. Phys. A: Atomic Nuclei* **334**, 269 (1989).
- [8] C. N. Davids and J. D. Larson, *Nucl. Instrum. Methods Phys. Res.* **B40/41**, 1224 (1989); C. N. Davids, B. B. Back, K. Bindra, D. J. Henderson, W. Kutschera, T. Lauritsen, Y. Nagame, P. Sugathan, A. V. Ramayya, and W. B. Walters, *ibid.* **B70**, 358 (1992).
- [9] A. J. Kreiner, C. Baktash, G. Garcia Bermudez, and M. A. J. Mariscotti, *Phys. Rev. Lett.* **47**, 1709 (1981).
- [10] G. J. Lane *et al.* (private communication).
- [11] W. Nazarewicz, *Phys. Lett. B* **305**, 195 (1993).